0026-895X/05/6803-830–839$20.00
MOLECULAR PHARMACOLOGY
Copyright © 2005 The American Society for Pharmacology and Experimental Therapeutics
Mol Pharmacol 68:830–839, 2005

Vol. 68, No. 3
12187/3048731
Printed in U.S.A.

Uridine Binding and Transportability Determinants of Human Concentrative Nucleoside Transporters

Jing Zhang, Kyla M. Smith, Tracey Tackaberry, Frank Visser, Morris J. Robins, Lars P. C. Nielsen, Ireneusz Nowak, Edward Karpinski, Stephen A. Baldwin, James D. Young, and Carol E. Cass

From the Departments of Oncology (J.Z., T.T., F.V., and C.E.C.) and Physiology (K.M.S., E.K., and J.D.Y.), Membrane Protein Research Group (J.Z., K.M.S., T.T., F.V., J.D.Y. and C.E.C.), University of Alberta, and the Cross Cancer Institute (J.Z., T.T., F.V. and C.E.C.), Edmonton, Alberta, Canada; the Department of Chemistry and Biochemistry, Brigham Young University, Provo, Utah (M.J.R., L.P.C.N., and I.N.); and the School of Biochemistry and Molecular Biology, University of Leeds, Leeds, United Kingdom (S.A.B.)

Received February 22, 2005; accepted June 14, 2005

ABSTRACT

Human concentrative nucleoside transporters 1, 2, and 3 (hCNT1, hCNT2, and hCNT3) exhibit different functional characteristics, and a better understanding of their permeant selectivities is critical for development of nucleoside analog drugs with optimal pharmacokinetic properties. In this study, the sensitivity of a high-throughput yeast expression system used previously for hCNT1 and hCNT3 was improved and used to characterize determinants for interaction of uridine (Urd) with hCNT2. The observed changes of binding energy between hCNT2 and different Urd analogs suggested that it interacts with C(3′)-OH, C(5′)-OH, and N(3)-H of Urd. The C(2′) and C(5) regions of Urd played minor but significant roles for Urd-hCNT2 binding, possibly through Van der Waals interactions. Because the yeast assay only provided information about potential transportability, the permeant selectivities of recombinant hCNT1, hCNT2, and hCNT3 produced in *Xenopus laevis* oocytes were investigated using a two-electrode voltage clamp assay. hCNT1-mediated transport was sensitive to modifications of the N(3), C(3′), and C(5′) positions of Urd. hCNT2 showed some tolerance for transporting Urd analogs with C(2′) or C(5) modifications, little tolerance for N(3) modifications, and no tolerance for any modifications at C(3′) or C(5′) of Urd. Although hCNT3 was sensitive to C(3′) modifications, it transported a broad range of variously substituted Urd analogs. The transportability profiles identified in this study, which reflected the binding profiles well, should prove useful in the development of anticancer and antiviral therapies with nucleoside drugs that are permeants of members of the hCNT protein family.

Mammalian nucleoside transporters are classified into two structurally and mechanistically unrelated protein families, the concentrative and equilibrative nucleoside transporters (CNTs and ENTs) (Baldwin et al., 1999; Cass et al., 1999). The ENTs transport a broad range of purine and pyrimidine nucleosides down their concentration gradients, whereas the CNTs couple uphill nucleoside transport to downhill sodium transport and, in the case of human (h)CNT3, to proton transport. Three hCNTs with different permeant selectivities have been identified by molecular cloning and functional expression in *Xenopus laevis* oocytes (Ritzel et al., 1997, 1998, 2001). hCNT1 and hCNT2 prefer pyrimidine nucleosides and purine nucleosides, respectively, although hCNT1 also transports adenosine and hCNT2 also transports uridine

This study was supported by the National Cancer Institute of Canada (to C.E.C and J.D.Y.), Alberta Cancer Board (to C.E.C. and J.D.Y.), and pharmaceutical company gift funds to Brigham Young University (to M.J.R.). C.E.C. is Canada Research Chair in Oncology, and J.D.Y. is Heritage Scientist of the Alberta Heritage Foundation for Medical Research. Studentship support was from the Canadian Institute of Health Research (to J.Z.), the Alberta Heritage Foundation for Medical Research (to J.Z. and F.V.), the Department of Oncology Endowed Studentship (to J.Z. and F.V.), and the Brigham Young University Undergraduate Research Fellowship (to L.P.C.N.).

Article, publication date, and citation information can be found at http://molpharm.aspetjournals.org.

doi:10.1124/mol.105.012187.

ABBREVIATIONS: CNT, concentrative nucleoside transporter; ENT, equilibrative nucleoside transporter; DMSO, dimethyl sulfoxide; h, human; CMM, complete minimal medium; IC_{50}, inhibitory concentration, 50%; K_i, inhibitory constant; ΔG^0, Gibbs free energy; PCR, polymerase chain reaction; TTBS, 0.2% Tween 20, Tris-buffered saline; FUrd, 5-fluorouridine; IUrd, 5-iodouridine; BrUrd, 5-bromouridine; MeUrd, 5-methyluridine; 3MeUrd, 3-methyluridine; dUrd, deoxyuridine; araU, 1-(β-D-arabinofuranosyl)uracil; xyloU, 1-(β-D-xylofuranosyl)uracil; ddUrd, dideoxyuridine; OMeUrd, *O*-methyluridine; AzdUrd, azidodeoxyuridine; 5′-CldUrd, chloro-5′-deoxyuridine; iPUrd, *O*-isopropylideneuridine; FdUrd, 5-fluoro-2′-deoxyuridine; BrdUrd, 5-bromo-2′-deoxyuridine; IdUrd, 5-iodo-2′-deoxyuridine; EtdUrd, 5-ethyl-2′-deoxyuridine; Thd, thymidine; AZT, 3′-azido-3′-deoxythymidine.

(Urd). hCNT3 transports a broad range of pyrimidine and purine nucleosides (Ritzel et al., 2001; Zhang et al., 2003). The ENTs seem to be expressed in most human cell types. In contrast, the CNTs are found primarily in specialized cell types, including renal and gastrointestinal epithelia (Ritzel et al., 1998, 2001; del Santo et al., 2001; Li et al., 2001; Ngo et al., 2001), suggesting an important role in absorption, secretion, distribution, and elimination of physiologic nucleosides and nucleoside drugs. hCNTs have also been observed in leukemic cells and a few cancer cell lines (Mackey et al., 1998; Ritzel et al., 2001; Garcia-Manteiga et al., 2003). Differences in tissue distribution and permeant selectivities of hCNTs suggest different nucleoside-transport capacities of various tissues and distinct physiological and pharmacological roles.

Nucleoside analogs are used clinically in the treatment of cancer and viral infections. Understanding the structural requirements for transporter binding and translocation of nucleosides should enable the design of more effective strategies for use of therapeutic nucleosides. In the absence of detailed structures for nucleoside transporter proteins, several experimental approaches have been used to define the structural requirements of nucleosides for interaction with the transporters (Patil et al., 2000; Lang et al., 2001, 2004; Chang et al., 2004). A study with human intestinal brush-border membrane vesicles suggested that the binding sites of hCNT1 and hCNT2 differentially interacted with analogs of their common permeants, Urd and adenosine (Patil et al., 2000). Using three-dimensional quantitative structure-activity relationships that were based on inhibition data obtained previously, this same group generated pharmacophore models in which the predominant determinants for ligand interaction were hydrogen bonding for hCNT2 and electrostatic and steric features for hCNT1 and hENT1 (Chang et al., 2004). In a study with stably transfected human cell lines, hCNT1 and hCNT2 exhibited different capacities for the binding of Urd and adenosine analogs with substituents on the ribosyl and/or base moieties (Lang et al., 2001, 2004). A high-throughput inhibitor-sensitivity assay in which recombinant hCNT1, hCNT3, hENT1, and hENT2 were produced in yeast was used to quantify the inhibitory effects of Urd analogs with systematic sugar modifications (Zhang et al., 2003; Vickers et al., 2004). A common observation in all of these inhibition studies was the importance of the 3′-hydroxyl group for high-affinity interaction of permeants and/or inhibitors with the transporters.

A deficiency of the approaches taken thus far to define the structural determinants for interaction of nucleoside analogs with the transporters is that they are based primarily on inhibition data. The current work was undertaken to extend our earlier inhibition studies of Urd-binding motifs with hCNT1 and hCNT3 (Zhang et al., 2003) to include hCNT2, which was not examined previously because of its low expression levels in the yeast strain initially used in the inhibition assay, and to determine the extent to which the inhibitory uridine analogs were also permeants. The original difficulty of hCNT2 production was circumvented by introducing the hCNT2-containing plasmid into a double knock-out yeast strain (*fui1*:HIS3) that lacked both Urd permease (FUI1) and uracil permease (FUR4). The binding motif of hCNT2 exhibited distinct features compared with hCNT1 and hCNT3. Because a high-affinity ligand might inhibit nucleoside transport without also being transported, two voltage-clamp experiments were performed in *X. laevis* oocytes to determine whether the Urd analogs that inhibited Urd transport were also permeants, thus defining the transportability profiles of hCNT1, hCNT2, and hCNT3. Each hCNT exhibited a distinct Urd transportability profile that was closely related to its permeant-binding profile.

Materials and Methods

Strains and Media. BY4742-YBR021W (MATα, his3, leu2, lys2, ura3, ΔFUR4), which contains a disruption in the gene encoding the endogenous uracil permease, FUR4, was purchased from the American Type Culture Collection (Manassas, VA) and used as the parental yeast strain to generate the double-permease knock-out strain *fui1*::HIS3. *fui1*::HIS3 was generated by deleting the *fui1* gene using the polymerase chain reaction (PCR)-mediated one-step gene disruption method (Winzeler et al., 1999). Other strains were generated by transformation of the yeast-*Escherichia coli* shuttle vector pYPGE15 (Brunelli and Pall, 1993) into *fui1*::HIS3 using a standard lithium acetate method (Ito et al., 1983).

The gene locus for FUI1 was disrupted by integration of the HIS3 expression cassette, encoding imidazoleglycerol-phosphate dehydratase (EC 4.2.1.19) into the coding region of the FUI1 gene to create *fui1*::HIS3. The *fui1*-disruption mutants were selected in a medium that lacked histidine but contained 500 μM FUrd. Because FUI1-mediated transport of FUrd leads to yeast death (Vickers et al., 2000), survival in 500 μM FUrd indicated the successful targeted integration of the HIS3 cassette into the yeast genome with disruption of the *fui1* gene. Three of the surviving yeast colonies and BY4742-YBR021W were then tested for their abilities to transport [^{3}H]uracil or [^{3}H]Urd in the presence and absence of either 5 or 10 mM nonradioactive uracil or Urd, respectively.

Yeast strains were maintained in complete minimal medium (CMM) containing 0.67% yeast nitrogen base (Difco, Detroit, MI), amino acids (as required to maintain auxotrophic selection), and 2% glucose (CMM/Glu). Agar plates contained CMM with various supplements and 2% agar (Difco). Plasmids were propagated in *E. coli* strain TOP10F′ (Invitrogen, Carlsbad, CA) and maintained in Luria broth with 100 μg/ml ampicillin.

DNA Manipulation and Plasmid Construction. To construct the deletion strain *fui1*::HIS3, two 71-mer oligonucleotide primers were synthesized (Invitrogen), each containing (3′ to 5′) 21 bases of homology to the HIS3 cassette, a unique 50-bp tag sequence that was complementary to the region (either upstream or downstream of the *fui1* open reading frame) being targeted (including the start or stop codon). The 71-mer primers were used to amplify the HIS3 gene cassette, which was contained in plasmid pJJ215 (a generous gift from Dr. B. Lemire, University of Alberta, Edmonton, AB, Canada). The amplified PCR products were transformed into BY4742-YBR021W using the lithium acetate method, and the resulting transformed yeast was selected by growing on agar plates that contained 500 μM FUrd but lacked histidine.

For *Saccharomyces cerevisiae* expression, the hCNT2 open reading frames were amplified from vectors (pCDNA3-hCNT2) by PCR using the following primers (restriction sites underlined): 5′-XbaI-hCNT2 (5′-CTG TCT AGA ATG GAG AAA GCA AGT GGA AG-3′), 3′-KpnI-hCNT2 (5′-CGA GGT ACC TCA GGC ACA GAC GGT ATT GTT GTA G-3′). The amplified open reading frames were inserted into pYPGE15 (a high copy number episomal yeast vector that expresses the inserted DNA constitutively under the transcriptional control of the phosphoglycerate kinase promoter) to generate pYPhCNT2. The PCR reactions were performed using *Pwo* polymerase (Roche Diagnostics, Indianapolis, IN), and the resulting PCR products were verified by DNA sequencing using an ABI PRISM 310 sequence detection system (Applied Biosystems, Foster City, CA).

Immunostaining of Yeast Membranes. Yeast membranes were prepared by a method described previously (Vickers et al., 2000) and subjected to SDS-polyacrylamide gel electrophoresis (Vickers et al., 1999), after which proteins were transferred to polyvinylidene fluoride membranes (Immobilon-P; Millipore Corporation, Billerica, MA). The transfer membranes were blocked overnight at 4°C, first in TTBS (0.2% Tween 20, Tris-buffered saline) containing 5% (w/v) skim milk powder and then in TTBS with antibodies against hCNT2 and 5% (w/v) skim milk powder. The membranes were then washed three times with TTBS, incubated with TTBS-containing species-specific horseradish-peroxidase secondary antibodies (Jackson ImmunoResearch Laboratories Inc., West Grove, PA) and 5% (w/v) skim milk powder, washed with TTBS, and visualized with enhanced chemiluminescence (ECL; Amersham Biosciences Inc., Piscataway, NJ) and autoradiography. Monoclonal antibodies against hCNT2 were raised by established methods (Jennings et al., 2001) against an immunogenic epitope that corresponded to residues 30 to 51 of hCNT2, a region predicted to be located in a large intracellular loop close to the amino terminus. The conjugated and unconjugated synthetic peptides were obtained from the Alberta Peptide Institute (Edmonton, AB, Canada).

Urd Uptake in Yeast-Producing Recombinant hCNT2. The uptake of [^{3}H]Urd, [^{3}H]adenosine, [^{3}H]cytidine, and [^{3}H]inosine (Moravek Biochemicals, Brea, CA) into logarithmically proliferating yeast was measured using a cell harvester as described previously (Vickers et al., 2002; Zhang et al., 2003). In brief, yeast was grown in CMM/Glu to an OD_{600} of 0.8 to 1.2, washed three times with fresh CMM/Glu, pH 7.4, and resuspended to an OD_{600} of 4 in CMM/Glu, pH 7.4. Fifty-microliter portions of CMM/Glu, pH 7.4, with [^{3}H]Urd and a test compound (if present) at twice the desired concentration were preloaded into 96-well plates. The transport assays were initiated by adding an equal volume of yeast suspension at an OD_{600} of 4 to the individual wells of the preloaded 96-well plates, which were placed on the semiautomated cell harvester (Micro96 Cell Harvester; Molecular Devices, Sunnyvale, CA). At graded time intervals, groups of transport reactions (usually 24) were terminated simultaneously by harvesting yeast on glass-fiber filters (Skatron Instruments) with continued washing with demineralized water to remove unincorporated permeant. The filter discs with yeast corresponding to a particular transport assay were placed into individual scintillation counting vials (one disc per vial) to which 5 ml of scintillation counting fluid (MP Biomedicals, Irvine, CA) was added. Scintillation vials were allowed to sit at room temperature overnight with shaking before analysis.

The binding of Urd and its analogs to recombinant hCNT2 was assessed by measuring their abilities to inhibit the uptake of [^{3}H]Urd in the "inhibitor-sensitivity" assay as follows. Yeast were incubated with graded concentrations of a particular test compound and 1 μM [^{3}H]Urd in CMM/Glu (pH 7.4) for 20 min, after which [^{3}H]Urd uptake was measured. All of the experiments were carried out in quadruplicate. The amount of [^{3}H]Urd associated with yeast in the presence of 10 mM nonradioactive Urd was also determined to quantify nonspecifically associated radioactivity, which was subtracted from total radioactivity for each transport assay. Data were fitted to theoretical inhibition curves by nonlinear regression to obtain IC_{50} values (concentrations that inhibited reactions by 50%). K_i (inhibitory constant) values were determined from the equation (Cheng and Prusoff, 1973) in which $K_i = IC_{50}/[1 + (L/K_m)]$ and L = [^{3}H]Urd concentration, which was always 1 μM. Gibbs free energy (ΔG^0) was calculated from $\Delta G^0 = -RT\ln(K_i)$, in which R is the gas constant and T is the absolute temperature. The thermodynamic stability of transporter-inhibitor complexes was quantitatively estimated from ΔG^0 as described elsewhere (de Koning and Jarvis, 2001).

Steady-State Electrophysiological Studies. hCNT1, hCNT2, or hCNT3 cDNA in pGEM-HE (Ritzel et al., 1997, 1998, 2001) was linearized with NheI and transcribed with T3 or T7 polymerase using the mMessage mMachine (Ambion, Austin, TX) transcription system. In vitro synthesized transcripts were injected into isolated mature stage VI oocytes from *X. laevis* as described previously (Smith et al., 2004). Mock-injected oocytes were injected with water alone.

Oocyte membrane currents were measured using a GeneClamp 500B oocyte clamp (Axon Instruments Inc., Union City, CA) in the two-electrode voltage clamp mode as described previously (Smith et al., 2004). All of the experiments were performed at room temperature (20°C), and oocytes were discarded if membrane potentials were unstable or more positive than −30 mV. The membrane potential was clamped at a holding potential of −50 mV, and Urd or Urd analogs were added at various concentrations. The sodium currents induced by 100 μM Urd were used as controls to compare the transportability of Urd analogs by recombinant hCNT1, hCNT2, and hCNT3. The concentrations of Urd analogs for electrophysiological studies were chosen based on their K_i values for inhibition of hCNT1 and hCNT3 (Zhang et al., 2003) and hCNT2 (this study) as determined in the inhibitor-sensitivity assay. The transport medium contained: 100 mM NaCl, 2 mM KCl, 1 mM $CaCl_2$, 1 mM $MgCl_2$, and 10 mM HEPES, pH 7.5. Current values are presented as the means ± S.E of three or more oocytes.

Urd Analogs. The structures of Urd and its analogs were given previously (Zhang et al., 2003; Vickers et al., 2004). The Urd analogs used in this study were either obtained from R.I. Chemical, Inc. (Orange, CA) or were synthesized as described by Zhang et al. (2003).

Stock solutions of test compounds were either prepared in water or dimethyl sulfoxide (DMSO) (Sigma-Aldrich Canada Ltd., Oakville, ON, Canada), and the final concentration of DMSO in transport reactions was 0.1% if DMSO was used as a solvent.

Results

Detection of Recombinant hCNT2 in Yeast Membranes. The production of recombinant hCNT2 in *S. cerevisiae* was verified by immunoblotting using anti-hCNT2 antibodies (Fig. 1A). A 75-kDa immunoreactive species was detected in membranes of pYPhCNT2-containing yeast and was not detected in membranes of pYPGE15-containing yeast (Fig. 1A). The electrophoretic mobilities of the detected proteins were consistent with the predicted molecular mass of hCNT2.

Urd Transport by Recombinant hCNT2 Produced in Yeast. The FUI1 and FUR4 double knock-out strain (*fui1*::HIS3) was confirmed by demonstrating that it was unable to transport either [^{3}H]Urd or [^{3}H]uracil. The parental strain (BY4742-YBR021W) exhibited Urd but not uracil transport activity (data not shown).

The time course for uptake of 1 μM [^{3}H]Urd into *fui1*::HIS3 that contained pYPGE15 was linear over extended periods (>30 min) and exhibited rates of 0.05 ± 0.01 and 0.04 ± 0.01 pmol/mg of protein/min in the presence and absence of 10 mM nonradioactive Urd, respectively (data not shown). When time courses for an influx of 1 μM [^{3}H]Urd were measured in the presence and absence of 10 mM nonradioactive Urd into *fui1*::HIS3 yeast that contained pYPhCNT2 (Fig. 1B), the time courses were linear for up to 30 min with mean rates (±S.E.) of 4.1 ± 0.09 and 0.05 ± 0.02 pmol/mg of protein/min, respectively, indicating the presence of functional hCNT2 in yeast plasma membranes. Urd transport rates were determined for all subsequent experiments using incubation times of 20 min for recombinant hCNT2 produced in yeast, thereby providing large signal-to-noise ratios and maintaining initial rates of uptake. Results from similar experiments with other ^{3}H-labeled nucleosides demonstrated that recombinant hCNT2 also transported adenosine, ino-

sine, and guanosine but not cytidine and Thd (data not shown), confirming that the permeant selectivity of recombinant hCNT2 produced in yeast was similar to that reported previously in cultured cells and *X. laevis* oocytes (Ritzel et al., 1998; Lang et al., 2001, 2004), thus providing a good model system for structure-function studies.

The experiments of Fig. 1C showed that recombinant hCNT2 had a moderate apparent affinity and capacity for Urd uptake (K_m = 29 ± 7 μM, V_{max} = 146 ± 11 pmol/mg of protein/min; mean ± S.E., n = 3). The K_m value of recombinant hCNT2 was slightly lower than the values obtained with *X. laevis* oocytes [40 ± 6 μM (Ritzel et al., 1998)] and cultured mammalian cells (Ritzel et al., 1998; Lang et al., 2001); these differences are believed to be the result of variations in post-translational modifications in different expression systems and/or differences in membrane lipid environment (Visser et al., 2005).

Interaction of Urd Analogs with Recombinant hCNT2: Inhibitor-Sensitivity Assays. To gain an understanding of the structural regions of Urd that interact with hCNT2, Urd analogs with modifications of the base and/or sugar moieties were tested systematically by assessing the concentration dependence of inhibition of transport of 1 μM Urd mediated by hCNT2. The inhibition of Urd uptake was assumed to be competitive because 1) the inhibitors tested were close structural analogs of Urd and 2) the transporter under study was most likely to be the sole source of interaction with the potential inhibitor. Representative concentration-effect curves of some of the analogs for inhibition of

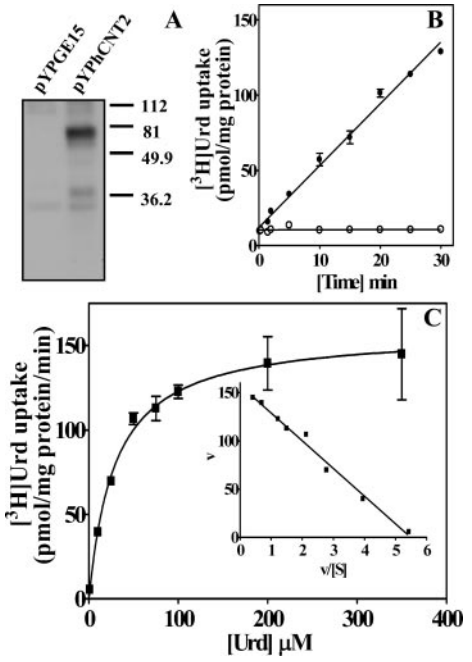

Fig. 1. Immunoblotting detection and functional characterization of recombinant hCNT2 in yeast. A, immunoblotting. Yeast (*fui1*::HIS3) were transformed with either pYPGE15 or pYPhCNT2 to form new yeast strains named *fui1*::HIS3 + pYPGE15 and *fui1*::HIS3 + pYPhCNT2. Yeast membranes (20 μg of protein) were subjected to SDS-polyacrylamide gel electrophoresis, after which proteins were transferred to polyvinylidene fluoride membranes that were subjected to immunoblotting with anti-hCNT2 monoclonal antibodies. The positions of the molecular mass markers are indicated in kilodaltons at the right. B, time courses of [³H]Urd uptake. The uptake of 1 μM [³H]Urd by yeast that was transformed with pYPhCNT2 was measured in CMM/Glu, pH 7.4, in the presence of 100 mM NaCl, either alone (closed symbols) or with 10 mM nonradioactive Urd (open symbols). C, kinetic properties. The mediated component of Urd transport (uptake rates of [³H]Urd at a particular Urd concentration minus uptake rates at that concentration in the presence of 10 mM nonradioactive permeants) was plotted as a function of concentration and subsequently converted to *V versus V/S* plots (insets) to determine the kinetic constants for hCNT2. Each value is the mean ± S.E. of nine determinations, and the mean ± S.E. values are not shown if they were smaller than the data points. Each graph represents one of three identical experiments that gave qualitatively similar results.

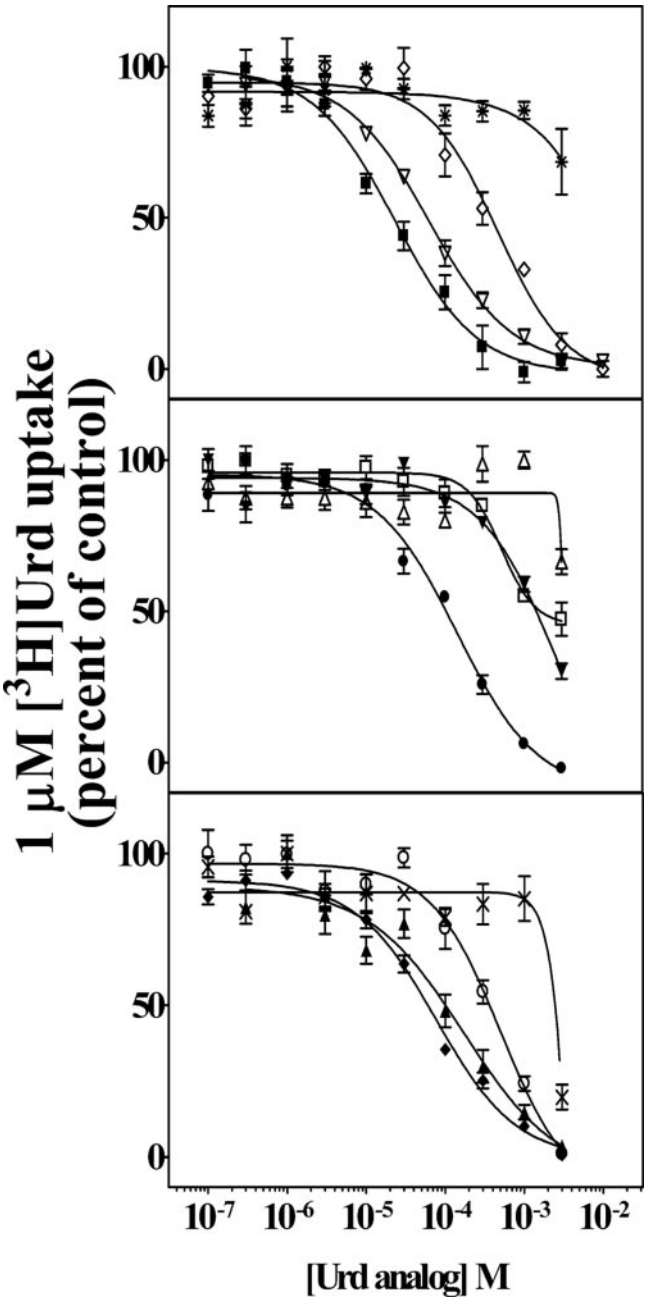

Fig. 2. Inhibition of recombinant hCNT2-mediated Urd uptake by some Urd analogs. The uptake of 1 μM [³H]Urd into *fui1*::HIS3 yeast-producing hCNT2 was measured over 20 min in the presence of graded concentrations of test compounds. The test compounds were as follows: Urd (■), 2′-dUrd (▽), 3′-dUrd (△), 5FUrd (♦), 3′-AzdUrd (*), FdUrd (●), EtdUrd (○), MeUrd (▲), IUrd (◇), 2′-AzdUrd (□), 2′-OMeUrd (+), and 5′-CldUrd (▼). Uptake values in the presence of Urd compounds are given as the percentage of uptake values in their absence. Each data point represents the means ± S.E. of quadruplicate determinations; error bars are not shown if they are smaller than the symbol. Three or four independent experiments gave similar results, and results from representative experiments are shown.

hCNT2-mediated Urd transport are shown in Fig. 2. In all cases, the Hill coefficients were close to −1 (mean ± S.E. = −0.9 ± 0.2), indicating a single class of inhibitor-binding sites. The mean K_i values (±S.E.) and the corresponding Gibbs free energy values are listed in Table 1.

Base Modifications. There were apparent weak interactions between hCNT2 and C(5) of Urd, because the addition of larger substituents at the C(5) position resulted in decreases of 2 to 6 kJ/mol in ΔG° with 2- to 15-fold increases in K_i values. The K_i values increased dramatically with the increase in volume of the substituent (e.g., fluoro < bromo < iodo) at C(5), FUrd exhibited a K_i value of 61 ± 13 μM, twice that of Urd (28 ± 3 μM), and IUrd exhibited a K_i value of 359 ± 50 μM, with a loss of 5.7 kJ/mol in ΔG^0, suggesting that the interactions between hCNT2 and C(5) were steric. Although these interactions were not tight, high concentrations of FUrd, IUrd, and BrdUrd were capable of completely inhibiting hCNT2-mediated transport of Urd. Thd was a weak inhibitor of Urd uptake with a K_i value of 566 ± 20 μM. The lower affinities for FdUrd, BrdUrd, IdUrd, and EtdUrd with ΔG^0 values of 8 to 20 kJ/mol compared with 2′-dUrd suggested that the ethyl and iodo substituents with larger sizes than the fluoro and bromo substituents may have sterically reduced the ability of the analog to efficiently contact the transporter protein.

The third position of the base moiety (N(3)-H) contributed a recognition determinant for binding to hCNT2. The low affinity of 3MeUrd, with a 20-fold increase in K_i value compared with that of Urd, indicated the importance of the N(3) position as part of the binding motif, with a difference of 7 kJ/mol binding energy, suggesting the loss of a weak hydrogen bond.

Sugar Modifications. hCNT2 displayed a reduced affinity for 2′-dUrd relative to Urd (Fig. 3), with a small loss of free energy [$\delta(\Delta G^0)$ = 2.1 kJ/mol]. However, C(2′) was an important determinant for high-affinity binding of Urd by hCNT2, because other modifications at this position reduced interactions with hCNT2. The inverted orientation of the hydroxyl group produced an analog that could no longer interact with hCNT2, because AraU, an epimer of Urd with the 2′-hydroxyl group above the plane of the sugar ring, exhibited a pronounced reduction in its interaction with the transporter (K_i > 3 mM). Compounds with substitution of an *O*-methyl or azido group for the 2′-hydroxyl group failed to inhibit hCNT2-mediated Urd transport at high concentrations (K_i > 3 mM), most probably because of the bulkier size of the C(2′)-*O*-CH_3 and C(2′)-N3 substituents.

Strong interactions existed between hCNT2 and C(5′)- and C(3′)-OH moieties, because the removal of either the 5′- or 3′-hydroxyl groups yielded K_i values >3 mM with losses of >10.5 kJ/mol in ΔG^0, suggesting that hydrogen bonding was important. Although 2′-dUrd was a moderate-affinity inhibitor of hCNT2-mediated Urd transport, additional removal of the 3′- or 5′-hydroxyl groups diminished its inhibitory effects.

TABLE 1

K_i and Gibbs free energy values for inhibition of hCNT2-mediated Urd uptake in *S. cerevisiae* by Urd analogs

The uptake of 1 μM [^{3}H]Urd into yeast (*fui1*::HIS3) expressing pYPhCNT2 was measured over 20 min in the presence of graded concentrations of nonradioactive Urd or Urd analogs. IC_{50} values (mean ± S.E., n = 3–4) were determined using Prism version 3.0 software (GraphPad Software Inc., San Diego, CA) and were converted to K_i values (Cheng and Prusoff, 1973) using K_m values (mean ± S.E., n = 3) of 29 ± 7 μM for recombinant hCNT2. ΔG^0 was calculated from $\Delta G^0 = -RT\ln(K_i)$.

Urd Compounds	IC_{50}	K_i	ΔG^0	$\delta(\Delta G^0)$
	μM			
Urd	29 ± 3	28 ± 3	23.8	0
Base modification				
FUrd	63 ± 13	61 ± 13	22.1	1.7
IUrd	371 ± 51	358 ± 50	18.1	5.7
BrUrd	238 ± 4	230 ± 4	19.1	4.7
MeUrd	165 ± 0.3	160 ± 1	19.9	3.9
3MeUrd	581 ± 151	562 ± 146	17.1	6.7
Sugar modification				
2′-dUrd	76 ± 8	73 ± 8	21.7	2.1
5′-dUrd	>3000[a]	>3000[a]	<13.3	>10.5
3′-dUrd	>3000[b]	>3000[b]		
araU	>3000[a]	>3000[a]		
xyloU	>3000[a]	>3000[a]		
2′,5′-ddUrd	>3000[a]	>3000[a]		
3′,5′-ddUrd	>3000[a]	>3000[a]		
2′,3′-ddUrd	>3000[b]	>3000[b]		
2′-OMeUrd	>1000[a]	>1000[a]	<15.8	>8.0
5′-OMeUrd	>3000[a]	>3000[a]		
3′-OMeUrd	>3000[a]	>3000[a]		
2′-AzdUrd	>3000[b]	>3000[b]		
3′-AzdUrd	>3000[a]	>3000[a]		
5′-AzdUrd	>3000[a]	>3000[a]		
5′-CldUrd	>1000[a]	>1000[a]		
iPUrd	>3000[a]	>3000[a]		
Base and sugar modifications				
FdUrd	156 ± 7	151 ± 7	20.0	3.8
BrdUrd	272 ± 75	263 ± 72	18.8	5.0
IdUrd	303 ± 20	293 ± 11	18.5	5.3
EtdUrd	353 ± 40	341 ± 39	18.2	5.6
5-Fluoro-5′-deoxyuridine	>3000[b]	>3000[b]		
Thd	586 ± 20	566 ± 20	17.0	6.8
AZT	>3000[b]	>3000[b]		

[a] No obvious inhibition was observed.
[b] Inhibition of <50% was observed.

The possible involvement of the 3′- and 5′-hydroxyl groups was also apparent from the effects of substitution of an azido or *O*-methyl group at these positions; hCNT2-mediated Urd transport remained unchanged in the presence of high concentrations of 3′-AzdUrd, 3′-OMeUrd, 5′-AzdUrd, or 5′-OMeUrd. AZT, which is 3′-azido-3′-deoxyothymidine, failed to inhibit hCNT2-mediated Urd uptake. The loss of more than 8 kJ/mol in ΔG^0 value upon substitution of a chloro group at the C(5′) of 5′-dUrd suggested the loss of hydrogen bonding between Urd and hCNT2. Although hCNT2 strongly bound Urd with the 3′-hydroxyl group below the sugar ring plane, its affinity for xyloU with the 3′-hydroxyl group oriented upward was greatly reduced ($K_i > 3$ mM). Likewise, iPUrd failed to inhibit Urd transport, presumably because of the presence at the 3′ position of the isopropylidene group.

Permeant Selectivities of hCNT1, hCNT2, and hCNT3 for Urd Analogs: Transport Assays. To determine whether the Urd analogs that bound to hCNT1 (Zhang et al., 2003), hCNT3 (Zhang et al., 2003), or hCNT2 (this study) were also permeants, two-electrode voltage clamp studies were used to measure their abilities to induce inward sodium currents in oocytes of *X. laevis* producing each of the transporters. Currents produced by Urd, 2′-dUrd, 3′-dUrd, and 5′-dUrd in a sodium-containing medium are shown in Fig. 3. Average current values for Urd analogs with base modifications observed in oocytes injected with transcripts are shown in Fig. 4. To compare the transportability of Urd and Urd analogs, the mean values of Urd analog-induced currents were normalized to the mean values of Urd-produced currents and summarized as I_{Analog}/I_{Urd} in Table 2 for hCNT1,

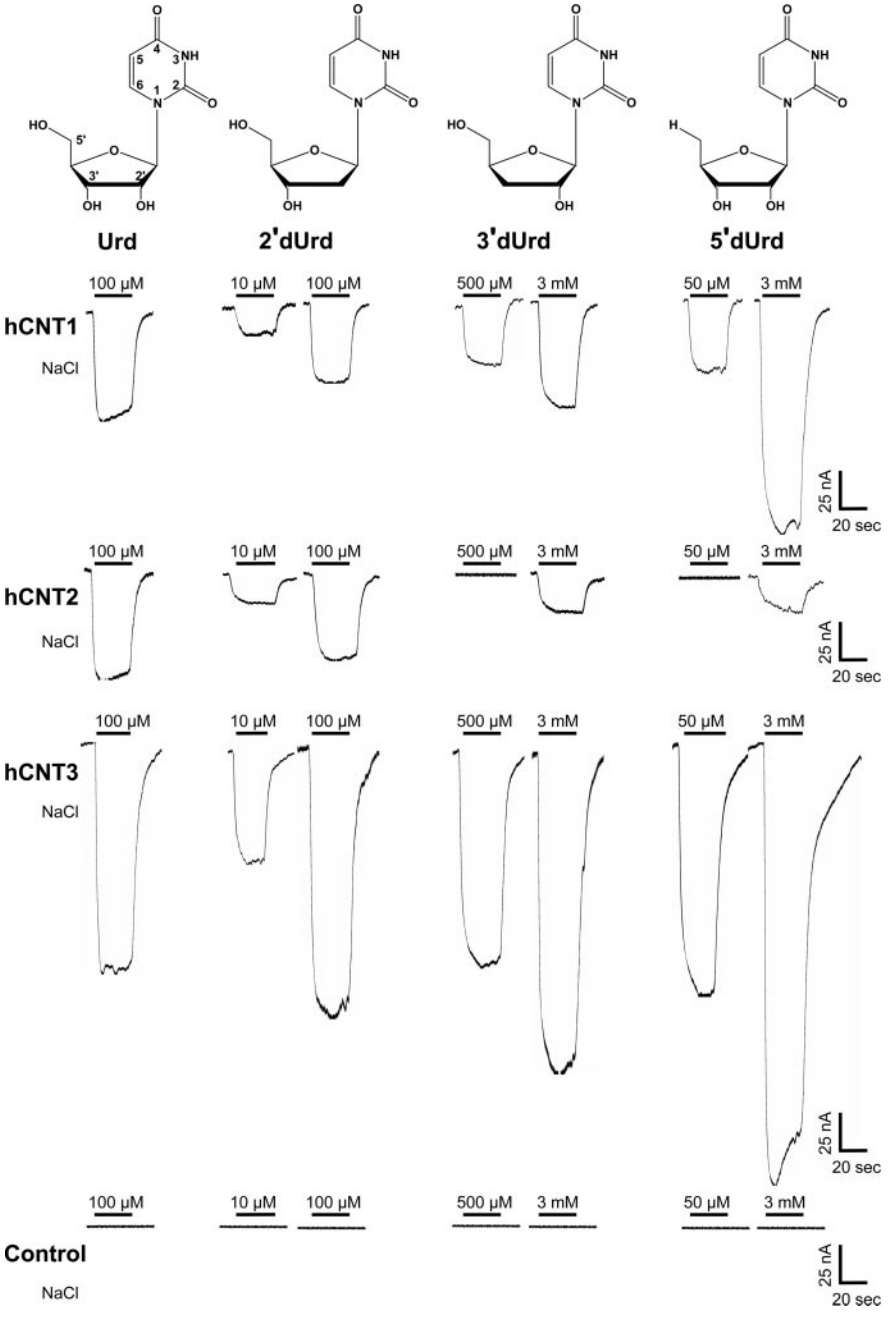

Fig. 3. Representative sodium currents in the presence of Urd, 2′-dUrd, 3′-dUrd, or 5′-dUrd. Oocytes were injected with 10 nl of water without (control) or with 10 ng of hCNT1, hCNT2, or hCNT3 transcripts. The expression vector was pGEM-HE. Current responses were generated by perfusing individual hCNT1-, hCNT2-, or hCNT3-producing oocytes with 2′-dUrd, 3′-dUrd, or 5′-dUrd with the concentrations as indicated in a sodium-containing transport medium (top three panels). The current produced by 100 μM Urd in a sodium-containing medium is shown for comparison. The same experiment was performed in a control water-injected oocyte (bottom). Structures were drawn using ChemDraw Ultra, version 6.0 software, and numbering for Urd is indicated.

hCNT2, and hCNT3. hCNT1 and hCNT2 generated similar inward currents (I_{Na} = 140 nA), whereas hCNT3 induced higher currents (I_{Na} = 330 nA) in the presence of 100 μM Urd. In all cases, the inward-directed sodium currents were reversible and abolished in a sodium-free medium, and no steady-state currents were observed in control water-injected oocytes (data not shown).

Base Modifications. Moderate currents (I_{Analog}/I_{Urd} = 20–60%) were elicited by hCNT1 and hCNT3 upon application of various concentrations of FUrd, IUrd, MeUrd, and BrUrd, whereas hCNT2 exhibited greatly reduced ability to transport Urd analogs with modifications at C(5) after a trend of diminished transportability with bulkier substituents [i.e., Urd (100 μM) > FUrd (50 and 100 μM) > MeUrd (500 μM) > IUrd and BrUrd (500 μM)]. Unlike hCNT1 and hCNT2, hCNT3 transported 3MeUrd well at higher concentrations (I_{Analog}/I_{Urd} = 48%, 500 μM 3MeUrd).

Sugar Modifications. Moderate to large inward currents were elicited by hCNT1 with application of 2′-dUrd or 5′-dUrd. The slightly higher currents of hCNT1 (I_{Analog}/I_{Urd} = 112%) observed with 2′,5′-ddUrd (100 μM) compared with that of Urd (100 μM) indicated that the 2′- and 5′-hydroxyl groups were not obligatory for transportability by hCNT1. The addition of an *O*-methyl group at the 2′ position resulted in a substantial decrease of sodium current; with a concentration of 1 mM, only 41% I_{Urd} induced by 100 μM Urd was observed with 2′-OMeUrd. Although hCNT1 was able to transport Urd analogs with different modifications at C(2′), including substitution of the hydroxyl group with an azido group (2′-AzdUrd), it barely transported AraU (I_{Analog}/I_{Urd} = 4.5%). hCNT1 exhibited high tolerance for substitution of the 5′-hydroxyl with chloro but lower tolerance for the other substitutions (e.g., replacement with an azido or *O*-methyl group yielded poor permeants with I_{Analog}/I_{Urd} values of less than 10% of that observed with Urd). 3′-dUrd initiated moderate to high inward currents at high concentrations (I_{Analog}/I_{Urd} = 91%, 3 mM 3′-dUrd, Fig. 3), and small but significant currents were induced by 3 mM 2′,3′-ddUrd, 3′,5′-ddUrd, 3′-AzdUrd, 3′-MedUrdU, and xyloU. No currents were observed in the presence of iPUrd.

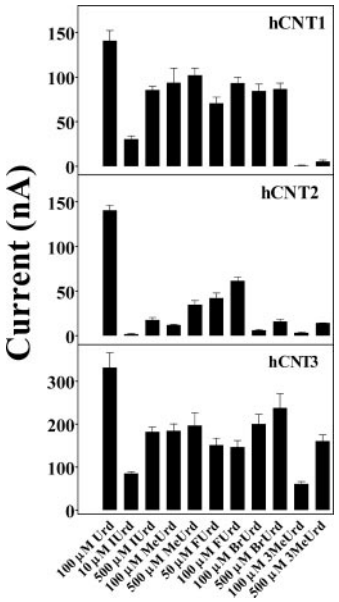

Fig. 4. Transport of Urd and Urd analogs by hCNT1, hCNT2, and hCNT3. Currents were generated by perfusing hCNT1-, hCNT2-, or hCNT3-producing oocytes with Urd or various Urd analogs with base modifications (concentrations as indicated) in a sodium-containing medium. Values are means ± S.E. for three different oocytes. The same experiment was also performed in control water-injected oocytes (data not shown); no inward currents were generated. The expression vector was pGEM-HE.

hCNT2 transported Urd analogs with modifications at the C(2′) position, whereas those with modification at the C(5′) and C(3′) positions were poorly transported, if at all. Moderate currents were produced by 100 μM 2′-dUrd, whereas only small currents were induced by 3 mM 5′-dUrd (I_{Analog}/I_{Urd} = 14.7%). We were surprised to observe that 2′,5′ddU, a poor permeant for hCNT2 at 100 μM (3.1% I_{Urd}), induced a current at a concentration of 3 mM, which was higher than that of 5′-dUrd. Likewise, although they were poor permeants at low concentrations, compounds with C(2′) modifications initiated significant inward currents at higher concentration (3 mM), with 2′-AzdUrd > 2′-OMeUrd > araU. C(5′) modifications significantly reduced transportability. hCNT2 transported 5′-CldUrd and 5′-AzdUrd poorly at high concentrations and was unable to transport 5′-OMeUrd. Small and moderate currents were induced with 500 μM and 3 mM 3′-dUrd, respectively (I_{Analog}/I_{Urd} = 4.2% at 500 μM versus 30.4% at 3 mM). Although weak currents were detected with 3 mM 2′,3′-ddUrd, no currents were initiated by hCNT2 with xyloU, 3′,5′-ddU, 3′-AzdUrd, 3′-OMeUrd, or iPUrd.

hCNT3 transported a broad range of Urd analogs. The absence of the 2′- and/or 5′-hydroxyl groups had no effect on transportability by hCNT3, because the sodium currents produced by 100 μM 2′-Urd, 5′-Urd, and 2′,5′-ddUrd were similar to that of Urd (Fig. 3). At 50 μM, the 2′-AzdUrd-induced current was similar to that induced by 100 μM Urd. However, hCNT3 showed reduced transportability of 2′-OMeUrd (I_{Analog}/I_{Urd} = 33.6% at 100 μM and 64.5% at 1 mM). Moderate inward currents were induced by 3 mM araU, suggesting that the translocation pore of hCNT3 is more flexible than the pores of hCNT1 and hCNT2. Urd analogs containing 5′ modifications, including 5′-CldUrd, 5′-AzdUrd, and 5′-OMeUrd, were good permeants with I_{Analog}/I_{Urd} of 29.0% for 10 μM 5′-CldUrd and approximately 70.0% for 5′-AzdUrd and 5′-OMeUrd. hCNT3 handled Urd analogs with 3′ modifications much better than hCNT1 and hCNT2. Large currents were induced by 3′-dUrd at 500 μM (I_{Analog}/I_{Urd} = 77.5%). At high concentrations (3 mM), 3′-dUrd (Fig. 3), 2′,3′-ddUrd, and xyloU produced moderate to large inward currents, whereas 3′-AzdUrd, 3′-OMeUrd, and iPUrd induced low currents and thus were poor permeants of hCNT3.

Base and Sugar Modifications. The hCNT1-mediated currents induced by FdUrd, BrdUrd, IdUrd, and EtdUrd (I_{Analog}/I_{Urd} = 50–70%) were similar to those induced by FUrd, BrUrd, and IUrd. The hCNT2-mediated current induced by FdUrd was reduced compared with that induced by 2′-dUrd (I_{Analog}/I_{Urd} = 32.8% for 100 μM FdUrd versus 75.5% for 100 μM 2′-dUrd); current was also induced by BrdUrd, whereas IdUrd and EtdUrd had almost no effect. FdUrd, BrdUrd, and IdUrd all induced moderate currents in hCNT3-producing oocytes. Lack of the 5′-hydroxyl group in 5-fluoro-5′-dUrd compared with 5FUrd had no effect on current induction in either hCNT1- or hCNT3-producing oocytes but resulted in dramatically decreased currents in hCNT2-producing oocytes. Thd and AZT induced large and moderate

currents, respectively, for hCNT1 and hCNT3 but very small or no currents for hCNT2.

Discussion

The present work used an improved yeast expression system to characterize the Urd-binding motif of hCNT2. Among the three hCNT proteins, hCNT2 showed the lowest affinity for Urd and was most sensitive to modifications of its structure. The regions of the sugar moiety most critical for interaction with hCNT2 were the C(3′)- and C(5′)-OH groups. Retention of these two hydroxyl groups was required for high-affinity interactions with hCNT2, because all modifications at C(3′) and C(5′) reduced the capacity of hCNT2 to bind Urd analogs. The critical region of the base moiety of Urd for binding was identified as N(3)-H. The loss of more than 10.5 and 6.7 kJ/mol in Gibbs free energy, respectively, when the 3′- or 5′-hydroxyl groups and the N(3)-H were removed or modified suggested that these groups were involved in hydrogen bonding with hCNT2. These findings

TABLE 2

The transportability of uridine analogs by hCNT1, hCNT2, and hCNT3 as measured by induction of sodium currents.

Oocytes producing hCNT1, hCNT2, or hCNT3 were voltage-clamped at −50 mV in a sodium-containing medium, and currents were measured in the presence of Urd analogs at different concentrations (three to four different oocytes per assay). The mean values of Urd analog-induced currents were normalized to the mean value of Urd-produced currents (100 μM Urd) and summarized as I_{Analog}/I_{Urd}. None of the Urd analogs induced currents in water-injected control oocytes (data not shown). The expression vector was pGEM-T.

Uridine Analogs	Concentration	I_{Analog}/I_{Urd} (% of Value Observed with 100 μM Urd)		
		hCNT1	hCNT2	hCNT3
	μM			
Urd	100	100 ± 8.0	100 ± 9.2	100 ± 14.4
Base modifications				
IUrd	10	21.5 ± 2.6	1.2 ± 0.6	25.6 ± 1.2
IUrd	500	60.6 ± 3.1	12.4 ± 2.1	54.9 ± 3.4
MeUrd	100	66.6 ± 11.5	8.5 ± 0.7	55.5 ± 4.8
MeUrd	500	72.5 ± 5.7	24.9 ± 3.2	59.3 ± 8.8
FUrd	50	50.2 ± 4.7	30.0 ± 4.0	45.6 ± 4.7
FUrd	100	66.3 ± 4.6	43.9 ± 3.0	44.2 ± 4.6
BrUrd	100	59.9 ± 5.6	4.3 ± 0.7	60.3 ± 6.9
BrUrd	500	61.6 ± 4.7	11.4 ± 1.6	71.8 ± 9.9
3MeUrd	100	0.5 ± 0.3	2.4 ± 0.6	4.6 ± 0.9
3MeUrd	500	3.8 ± 1.2	10.2 ± 0.2	48.4 ± 4.4
Sugar modifications				
2′-dUrd	10	18 ± 3.6	16.8 ± 2.1	30.5 ± 2.5
2′-dUrd	100	62.1 ± 9.0	75.5 ± 10.4	99.9 ± 7.8
5′-dUrd	50	39.6 ± 6.3	1.0 ± 0.7	85.4 ± 3.5
5′-dUrd	3000	218.9 ± 18.9	14.7 ± 2.1	150.9 ± 6.0
3′-dUrd	500	39.6 ± 4.5	4.2 ± 2.0	75.4 ± 4.6
3′-dUrd	3000	91 ± 9.9	30.4 ± 6.3	107.3 ± 6.4
AraU	3000	4.5 ± 1.8	13.6 ± 1.5	52.1 ± 2.5
XyloU	3000	9.9 ± 1.8	0	62.3 ± 3.9
2′,5′-ddUrd	100	111.7 ± 7.2	3.1 ± 1.2	100.9 ± 4.6
2′,5′-ddUrd	3000	166.6 ± 12.6	46.2 ± 7.3	117.6 ± 14.6
3′,5′-ddUrd	3000	11.7 ± 2.7	0	29.8 ± 3.2
2′,3′-ddUrd	3000	54.9 ± 12.6	2.1 ± 1.0	87.8 ± 6.0
2′-OMeUrd	100	23.4 ± 3.6	5.2 ± 1.2	33.6 ± 3.9
2′-OMeUrd	1000	41.4 ± 5.4	29.4 ± 5.3	64.5 ± 5.7
5′-OMeUrd	100	8.1 ± 2.7	0	63.0 ± 8.1
5′-OMeUrd	3000	46.8 ± 5.4	0	79.0 ± 10.2
3′-OMeUrd	3000	4.5 ± 1.8	0	12.0 ± 1.1
2′-AzdUrd	50	28.8 ± 7.2	8.4 ± 2.0	75.8 ± 3.9
2′-AzdUrd	3000	N.D.	39.9 ± 4.2	N.D.
3′-AzdUrd	1000	0	N.D.	6.4 ± 1.4
3′-AzdUrd	3000	3.6 ± 1.8	0	16.3 ± 2.5
5′-AzdUrd	100	9.0 ± 2.7	N.D.	78.6 ± 4.3
5′-AzdUrd	3000	N.D.	25.2 ± 3.1	N.D.
5′-CldUrd	10	18.9 ± 1.8	0	29.0 ± 1.8
5′-CldUrd	1000	149.5 ± 11.7	31.5 ± 8.4	147.7 ± 10.6
IPUrd	3000	0	0	2.5 ± 0.7
Base and sugar modifications				
FdUrd	10	22.2 ± 1.4	4.4 ± 0.5	31.8 ± 5.5
FdUrd	100	72.3 ± 5.0	32.8 ± 4.7	81.3 ± 18.8
BrdUrd	10	20.3 ± 2.4	2.1 ± 0.6	23.4 ± 3.2
BrdUrd	500	56.3 ± 9.0	32.6 ± 7.0	N.D.
IdUrd	100	72.1 ± 3.8	1.0 ± 0.3	54.9 ± 6.2
EtdUrd	50	51.4 ± 4.1	0.3 ± 0.3	51.5 ± 3.1
EtdUrd	500	113.5 ± 11.8	2.3 ± 0.1	70.6 ± 2.5
5-Fluoro-5′-dUrd	50	33.4 ± 0.8	0.0	37.7 ± 2.0
5-Fluoro-5′-dUrd	3000	N.D.	12.4 ± 2.1	N.D.
Thd	100	83.2 ± 2.8	4.1 ± 1.4	63.1 ± 10.6
AZT	100	19.2 ± 1.7	0.0	8.5 ± 1.3
AZT	1000	59.9 ± 6.5	0.0	28.1 ± 3.2

N.D., not determined.

were consistent with the predictions of a recent computer-based pharmacophore model for nucleoside-hCNT2 binding, which suggested that hydrogen bonding was a dominant determinate of interaction between hCNT2 and nucleosides (Chang et al., 2004).

The C(2′) and C(5) positions were important regions for hCNT2 binding. hCNT2 tolerated the removal of the 2′-hydroxyl group but not its inversion of configuration or substitution with an azido or an *O*-methyl group. Considerable steric interference and physical separation introduced by modifications evidently weakened permeant-transporter interactions. Weak interactions, probably through Van der Waals forces, existed between hCNT2 and the C(5) position of the base moiety. The addition of halogen, methyl, or ethyl groups to the C(5) regions of Urd and 2′-dUrd resulted in similar affinity losses roughly corresponding to the volume size of the modifications.

Although the structural regions of Urd that were involved in binding to hCNT2 shared similarities with those of hCNT1 and hCNT3, distinguishable features of hCNT2-Urd interactions were observed. We established previously that the 3′-hydroxyl is the single most critical functional group of Urd for high-affinity binding by hCNT1 and hCNT3 (Zhang et al., 2003); in this study, we have found that both the 5′- and 3′-hydroxyl moieties were critical for hCNT2 binding. The C(2′) and C(5) positions, which were relatively unimportant for hCNT1 or hCNT3 binding of Urd, were the second most important regions for hCNT2-Urd interactions. Multiple regions are required for direct or indirect hCNT2 interaction with Urd, suggesting that the amino acid residues composing the nucleoside-binding pocket of hCNT2 have limited selectivity for pyrimidine nucleosides.

Because the structural determinants of Urd that were identified by the inhibitor-sensitivity assay might not be equivalent to those required for physical translocation across the membrane by the hCNT proteins, the two-voltage clamp assay was used to determine the regions of Urd that were important for hCNT transportability in the *X. laevis* oocyte expression system. The regions of Urd required for hCNT1-mediated transport were identified as C(5), N(3), and C(3′). The transportability of Urd analogs depended on both the structural region(s) and the nature of the modifications. Urd analogs with C(5) modifications, which were high-affinity inhibitors of hCNT1 (Zhang et al., 2003), were also good permeants. It is noteworthy that a Urd analog with equal or even higher affinity than Urd did not necessarily produce higher currents than Urd. For example, hCNT1 exhibited significantly higher affinities for binding and transport of FUrd and FdUrd, because the apparent K_i and K_m values of FUrd and FdUrd were smaller than those of Urd (Zhang et al., 2003; Smith et al., 2004); however, the currents induced by these two permeants were smaller than those induced by Urd. Methylation of N(3) reduced interactions with hCNT1, because the latter exhibited decreased affinity and greatly reduced transportability of 3MeUrd. C(2′)-OH was not a determinant for hCNT1-Urd interactions, because Urd analogs with modifications at this position were both good inhibitors (Zhang et al., 2003) and permeants of hCNT1. The 5′-hydroxyl group, which was previously identified as a potential H-bond donor for high-affinity hCNT1-Urd interactions (Zhang et al., 2003), was not important for transport by hCNT1, because 5′-dUrd and 5′-CldUrd remained good permeants. However, 5′-AzdUrd and 5′-OMeUrd were not transported well by hCNT1, indicating that the 5′ region of the sugar moiety contributes to permeant selectivity. Modifications at C(3′) dramatically decreased the transportability of Urd analogs. hCNT1 was able to transport 3′-dUrd and 2′,3′-ddUrd at very high concentrations but was unable to transport Urd analogs with bulkier C(3′) substituents.

The transportability profile of hCNT2 corresponded well to its binding motif. Changes in almost all regions of Urd affected hCNT2 permeant selectivity. The most critical functional groups for binding to hCNT2 (i.e., the 3′- and 5′-hydroxyl groups) were also required for transportability. Almost any changes at the 3′ or 5′ positions, including removal of the hydroxyl group or inversion of configuration (at the 3′ position), modification, or substitution, yielded Urd analogs that were poor permeants or not permeants at all. hCNT2 showed moderate affinity for 2′-dUrd and also accepted 2′-dUrd as a good permeant. Substitution of a variety of groups for the 2′-hydroxyl group yielded Urd analogs with poor binding in hCNT2-producing yeast and poor transport in hCNT2-producing oocytes. The N(3) region of Urd was also a determinant of transportability. The small volume of the C(5) region was evidently needed for tight binding and efficient transport, because substitution of H with bulkier groups resulted in a similarly large loss of both binding and transport.

The C(3′), C(5), and N(3) regions of Urd affected hCNT3 to different degrees. A potential hydrogen-bond interaction at C(3′) of Urd was important for high-affinity binding and transport, because removal or modification of the 3′-hydroxyl group significantly reduced analog binding and weakened transport. However, most poor inhibitors of hCNT3 protein seemed to be transported at high concentrations. The C(2′) and C(5′) regions of Urd, which were shown previously to be unimportant for Urd binding, were not important for transport, because the C(2′)- and C(5′)-Urd analogs were also good permeants of hCNT3. Although modifications of C(5) and N(3) caused no substantial changes in binding to hCNT3 (Zhang et al., 2003), the corresponding Urd analogs were transported less well than either Urd or 2′dUrd, suggesting that these two regions were minor determinants for hCNT3 transportability.

The transportability of Urd analogs by hCNT1, hCNT2, and hCNT3 reflected well the results obtained in the inhibitor-sensitivity assays. Most, if not all, of the Urd analogs that inhibited hCNT1-, hCNT2-, or hCNT3-mediated Urd transport were also permeants. hCNT2, which showed the least tolerance for modifications of Urd in the inhibitor-sensitivity assay, also exhibited limited transport of Urd analogs in the sodium flux assay. In contrast, hCNT3, with the 3′-hydroxyl group being the only important structural determinant for binding, showed good tolerance to various modifications of Urd with respect to transportability.

In summary, an improved yeast expression system was developed and used to determine the Urd-binding motif of hCNT2, after which Urd analogs were applied to evaluate the transportability profiles of inhibitors of hCNT1, hCNT2, and hCNT3 with the two-electrode voltage clamp assay in oocytes of *X. laevis*. The transporters displayed key differences in their ligand recognition and permeant selectivities, indicating differences in permeant-binding and translocation sites. Although they are poor inhibitors, 3′-dUrd, 2′,3′-ddUrd,

3′,5′-ddUrd, araU, xyloU, and AZT were permeants for hCNT1 and hCNT3 at high concentrations, indicating the important roles of these transporters for delivery and distribution of nucleoside analogs. The results of this work will guide the rational design of nucleoside drugs for use in the treatment of human diseases.

Acknowledgments

We thank Pat Carpenter for excellent technical assistance.

References

Baldwin SA, Mackey JR, Cass CE, and Young JD (1999) Nucleoside transporters: molecular biology and implications for therapeutic development. *Mol Med Today* **5:**216–224.

Brunelli JP and Pall ML (1993) A series of yeast/*Escherichia coli* l expression vectors designed for directional cloning of cDNAs and *cre/lox*-mediated plasmid excision. *Yeast* **9:**1309–1318.

Cass CE, Young JD, Baldwin SA, Cabrita MA, Graham KA, Griffiths M, Jennings LL, Mackey JR, Ng AML, Ritzel MWL, et al. (1999) Nucleoside transporters of mammalian cells, in *Membrane Transporters as Drug Targets* (Amidon GL and Sadee W eds), pp 313–352, Kluwer Academic/Plenum Publishers, Zurich, Switzerland.

Chang C, Swaan PW, Ngo LY, Lum PY, Patil SD, and Unadkat JD (2004) Molecular requirements of the human nucleoside transporters hCNT1, hCNT2, and hENT1. *Mol Pharmacol* **65:**558–570.

Cheng Y and Prusoff WH (1973) Relationship between the inhibition constant (K_i) and the concentration of inhibitor which causes 50 percent inhibition (I_{50}) of an enzymatic reaction. *Biochem Pharmacol* **22:**3099–3108.

de Koning HP and Jarvis SM (2001) Uptake of pentamidine in *Trypanosoma brucei* brucei is mediated by the P2 adenosine transporter and at least one novel, unrelated transporter. *Acta Trop* **80:**245–250.

del Santo B, Tarafa G, Felipe A, Casado FJ, and Pastor-Anglada M (2001) Developmental regulation of the concentrative nucleoside transporters CNT1 and CNT2 in rat liver. *J Hepatol* **34:**873–880.

Garcia-Manteiga J, Molina-Arcas M, Casado FJ, Mazo A, and Pastor-Anglada M (2003) Nucleoside transporter profiles in human pancreatic cancer cells: role of hCNT1 in 2′,2′-difluorodeoxycytidine-induced cytotoxicity. *Clin Cancer Res* **9:**5000–5008.

Ito H, Fukuda Y, Murata K, and Kimura A (1983) Transformation of intact yeast cells treated with alkali cations. *J Bacteriol* **153:**163–168.

Jennings LL, Hao C, Cabrita MA, Vickers MF, Baldwin SA, Young JD, and Cass CE (2001) Distinct regional distribution of human equilibrative nucleoside transporter proteins 1 and 2 (hENT1 and hENT2) in the central nervous system. *Neuropharmacology* **40:**722–731.

Lang TT, Selner M, Young JD, and Cass CE (2001) Acquisition of human concentrative nucleoside transporter 2 (hcnt2) activity by gene transfer confers sensitivity to fluoropyrimidine nucleosides in drug-resistant leukemia cells. *Mol Pharmacol* **60:**1143–1152.

Lang TT, Young JD, and Cass CE (2004) Interactions of nucleoside analogs, caffeine, and nicotine with human-concentrative nucleoside transporters 1 and 2 stably produced in a transport-defective human cell line. *Mol Pharmacol* **65:**925–933.

Li JY, Boado RJ, and Pardridge WM (2001) Differential kinetics of transport of 2′,3′-dideoxyinosine and adenosine via concentrative Na^+ nucleoside transporter CNT2 cloned from rat blood-brain barrier. *J Pharmacol Exp Ther* **299:**735–740.

Mackey JR, Mani RS, Selner M, Mowles D, Young JD, Belt JA, Crawford CR, and Cass CE (1998) Functional nucleoside transporters are required for gemcitabine influx and manifestation of toxicity in cancer cell lines. *Cancer Res* **58:**4349–4357.

Ngo LY, Patil SD, and Unadkat JD (2001) Ontogenic and longitudinal activity of Na^+-nucleoside transporters in the human intestine. *Am J Physiol* **280:**G475–G481.

Patil SD, Ngo LY, and Unadkat JD (2000) Structure-inhibitory profiles of nucleosides for the human intestinal N1 and N2 Na^+-nucleoside transporters. *Cancer Chemother Pharmacol* **46:**394–402.

Ritzel MW, Yao SY, Huang MY, Elliott JF, Cass CE, and Young JD (1997) Molecular cloning and functional expression of cDNAs encoding a human Na^+-nucleoside cotransporter (hCNT1). *Am J Physiol* **272:**C707–C714.

Ritzel MW, Yao SY, Ng AM, Mackey JR, Cass CE, and Young JD (1998) Molecular cloning, functional expression, and chromosomal localization of a cDNA encoding a human Na^+/nucleoside cotransporter (hCNT2) selective for purine nucleosides and uridine. *Mol Membr Biol* **15:**203–211.

Ritzel MWL, Ng AM, Yao SYM, Graham K, Loewen SK, Smith KM, Ritzel RG, Mowles DA, Carpenter P, Chen X, et al. (2001) Molecular identification and characterization of novel human and mouse concentrative Na^+-nucleoside cotransporter proteins (hCNT3 and mCNT3) broadly selective for purine and pyrimidine nucleosides (system *cib*). *J Biol Chem* **276:**2914–2927.

Smith KM, Ng AM, Yao SY, Labedz KA, Knaus EE, Wiebe LI, Cass CE, Baldwin SA, Chen XZ, Karpinski E, et al. (2004) Electrophysiological characterization of a recombinant human Na^+-coupled nucleoside transporter (hCNT1) produced in *Xenopus* oocytes. *J Physiol* (*Lond*) **558:**807–823.

Vickers MF, Kumar R, Visser F, Zhang J, Charania J, Raborn RT, Baldwin SA, Young JD, and Cass CE (2002) Comparison of the interaction of uridine, cytidine, and other pyrimidine nucleoside analogues with recombinant human equilibrative nucleoside transporter 2 (hENT2) produced in *Saccharomyces cerevisiae. Biochem Cell Biol* **80:**639–644.

Vickers MF, Mani RS, Sundaram M, Hogue DL, Young JD, Baldwin SA, and Cass CE (1999) Functional production and reconstitution of the human equilibrative nucleoside transporter (hENT1) in *Saccharomyces cerevisiae*. Interaction of inhibitors of nucleoside transport with recombinant hENT1 and a glycosylation-defective derivative (hENT1/N48Q). *Biochem J* **339:**21–32.

Vickers MF, Yao SY, Baldwin SA, Young JD, and Cass CE (2000) Nucleoside transporter proteins of *Saccharomyces cerevisiae*. Demonstration of a transporter (FUI1) with high uridine selectivity in plasma membranes and a transporter (FUN26) with broad nucleoside selectivity in intracellular membranes. *J Biol Chem* **275:**25931–25938.

Vickers MF, Zhang J, Visser F, Tackaberry T, Robins MJ, Nielsen LP, Nowak I, Baldwin SA, Young JD, and Cass CE (2004) Uridine recognition motifs of human equilibrative nucleoside transporters 1 and 2 produced in *Saccharomyces cerevisiae. Nucleosides Nucleotides Nucleic Acids* **23:**361–373.

Visser F, Zhang J, Raborn RT, Baldwin SA, Young JD, and Cass CE (2005) Residue 33 of human equilibrative nucleoside transporter 2 is a functionally important component of both the dipyridamole and nucleoside-binding sites. *Mol Pharmacol* **67:**1291–1298.

Winzeler EA, Shoemaker DD, Astromoff A, Liang H, Anderson K, Andre B, Bangham R, Benito R, Boeke JD, Bussey H, et al. (1999) Functional characterization of the *S. cerevisiae* genome by gene deletion and parallel analysis. *Science (Wash DC)* **285:**901–906.

Zhang J, Visser F, Vickers MF, Lang T, Robins MJ, Nielsen LP, Nowak I, Baldwin SA, Young JD, and Cass CE (2003) Uridine binding motifs of human concentrative nucleoside transporters 1 and 3 produced in *Saccharomyces cerevisiae. Mol Pharmacol* **64:**1512–1520.

Address correspondence to: Dr. Carol E. Cass, Department of Oncology, University of Alberta, Cross Cancer Institute, 11540 University Ave., Edmonton, Alberta, Canada T6H 1Z2. E-mail: carol.cass@cancerboard.ab.ca